Quantum interference effects in two-photon spectroscopy*

M. M. Salour

Department of Physics and Gordon McKay Laboratory, Harvard University, Cambridge, Mass. 02138

Interaction of atoms with two intense coherent time-delayed short pulsed standing waves produces quantum interference effects in the atomic fluorescence. This type of quantum interference effect applied to Doppler-free two-photon spectroscopy (an extension of the Ramsey method of separated r.f. or microwave fields in atomic beam experiments) offers a number of important improvements in the presently available techniques of ultra-high-resolution spectroscopy of atoms, molecules, and crystals.

CONTENTS

I. INTRODUCTION

Interaction of atoms and molecules with intense monochromatic laser standing waves can give rise to very narrow Doppler-free two-photon resonances. This new high-resolution spectroscopic technique has recently been extensively applied to the study of various atomic and molecular optical transitions (Vasilenko *et al.*, 1970; Cagnac *et al.*, 1973, 1974; Levenson and Bloembergen, 1974; Hänsch *et al.*, 1974; Salour, 1976b; Woerdman, 1976). The principle of this technique is shown in Fig. 1. An atom is placed in a standing field wave [i.e., two light beams, beam 1 and beam 2, propagating in opposite directions, but having the same frequency; in the rest frame of the atom the frequency of beam 1 is $\nu(1-v/c)$, while the frequency of beam 2 is $\nu(1+v/c)$]. When the frequency ν of the light wave is tuned so that $2h\nu$ corresponds exactly to the energy difference between two sharp energy levels of the atom which have the same parity, the atom may undergo the two-photon transition in two ways:

First, the two photons may both be absorbed from either beam 1 or beam 2. The resulting energy is $2h\nu(1\pm v/c)$. Thus, the resonant frequency ν is shifted by the velocity v of the moving atom. This process produces a broad absorption peak which is much wider than the natural linewidth of the transition.

Second, the atom may absorb one photon from each of the beams. Then the resulting energy is $h\nu(1+v/c)+h\nu(1-v/c)=2h\nu$. Since this energy is velocity independent, all atoms, regardless of their velocity, will participate in resonance, and, more importantly, the linewidth of the transition can in theory be the natural linewidth of the radiating atoms.

Compared to other methods of precision spectroscopy, the Doppler-free two-photon technique offers some unique characteristics. These are:

(1) The initial and final states have the same parity. Furthermore, the final state may have an excitation energy in the far uv, while the incident light beam has a frequency in the near uv or blue part of the spectrum. These features make it possible to reach states which cannot be reached from the same initial state in a one-photon process.

(2) As was shown earlier, in Doppler-free two-photon spectroscopy, all atoms participate in the resonance, irrespective of their velocity. Furthermore, the probability amplitude for absorbing two counter propagating photons is proportional to $e^{i(\omega t-kz)}e^{i(\omega t+kz)}=e^{i2\omega t}$ and does not depend on the spatial position z of the atoms.

In the past few decades, great progress has been made in generating and measuring extremely narrow resonance lines at wavelengths longer and shorter than those of light. In the microwave-radio region of the spectrum, for example, a technique has been developed to generate narrow resonance lines with the aid of molecular beams. An arrangement consisting of two spatially separated

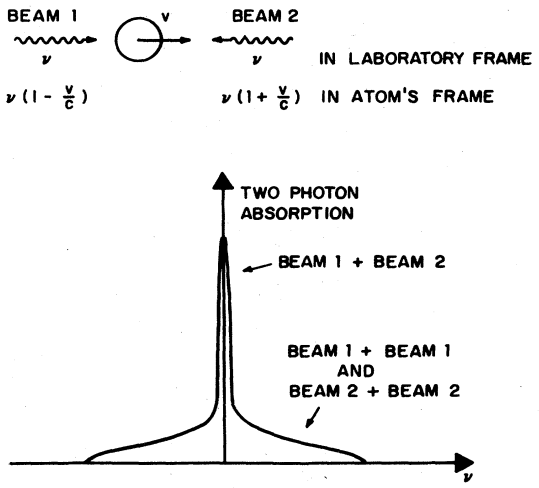

FIG. 1. Two-photon interaction frequencies and two-photon absorption line shape.

*Supported in part by Joint Services Electronic program.

[1]The method of using two coherent time delayed electromagnetic pulses has also been used in the microwave domain. See, e.g., Alley (1960); Arditi and Carber (1964).

microwave fields interacting with a beam of cesium atoms can produce resonances between a particular pair of hyperfine energy levels of the cesium atom that are 50 Hz wide at a frequency of about 9300 MHz (Ramsey, 1949, 1956). The accuracy of this measurement corresponds to a relative linewidth of approximately five parts in 10^9. (The relative linewidth is the ratio of the actual width of the spectral line to the center frequency of the resonance.) Narrow resonances of this kind provide the basis for the atomic scale of time used today throughout the world.

Advances have also been made in the gamma-ray region of the spectrum. Rudolf Mössbauer (1958a, 1958b, 1959) discovered that extremely narrow resonances can be produced in transitions between certain energy levels of atomic nuclei embedded in a crystal lattice. These resonance lines, the narrowest known at present, allow physical measurements to be made with an accuracy of one part in 10^{16} (Pound and Snider, 1965).

Thus techniques for producing extremely narrow resonance lines have been developed in both the low-frequency and the high-frequency ends of the electromagnetic spectrum. Until recently, however, little progress was made in achieving such narrow resonances in the intermediate spectral range, which spans the optical and infrared frequencies. Here the narrowest relative linewidths available were only about one part in 10^6. The introduction of the laser as a spectroscopic tool not only led to an important improvement in this figure by several orders of magnitude, but also, by its use as an intense, coherent light source, made possible the resolution of relative linewidths in the optical and infrared spectral regions to an accuracy of better than one part in 10^{13}, through methods of precision spectroscopy [such as saturation or two-photon techniques (Hartig and Walther, 1973; Grove *et al.*, 1973; Feld and Letokhov, 1973; Snyder and Hall, 1975)].

The ultimate resolution achievable by the method of Doppler-free two-photon spectroscopy is limited in principle only by the natural linewidth of the excited state; in practice, however, the observed linewidth has thus far been limited by the laser. Thus in order to take full advantage of the elimination of the Doppler width, the spectral linewidth of the laser light must be as small as possible, which explains the motivation for using cw lasers. But, on the other hand, two-photon resonances require an appreciable intensity, and it is well known that pulsed dye lasers deliver higher powers and, furthermore, cover a broader spectral range. Recently, by using pulsed dye lasers pumped with an N_2 laser, it has been possible to observe two-photon resonances in several highly excited states of various atomic vapors which could not have been reached by cw excitation (Salour, 1976b, 1978). The resolution was limited by the spectral width $1/\tau$ of the pulse (τ: duration of each pulse), thus making it impossible to resolve many closely spaced two-photon resonance lines.

II. QUANTUM INTERFERENCE

In an attempt to achieve the higher resolution associated with the two-photon resonances when a pulsed laser is used, we will demonstrate in this paper that, by exciting atoms with two time-delayed coherent laser pulses, one can obtain interference fringes in the profile of the Doppler-free two-photon resonances with a splitting $1/2T$ (T: delay between the two pulses) much smaller than the spectral width $1/\tau$ (τ: duration of each pulse). This technique combines the advantages of pulsed dye lasers (power, spectral range) with the high resolution usually associated with a cw excitation. Our experiment can be considered as an extension to two-photon Doppler-free resonances in the optical range of the well-known Ramsey method of using two separated rf or microwave fields in atomic beam experiments (Ramsey, 1949, 1956; Clark *et al.*, 1977).

Such an idea was first suggested in a slightly different context by Baklanov *et al.* (1976a, 1976b; and Dubetskii, 1976), who proposed using two spatially separated cw light standing waves. These authors considered two-photon Doppler-free resonances between two very sharp levels, such as ground states or metastable states (an important example being the $1S_{1/2} - 2S_{1/2}$ transition of H). In such a case, the use of a single laser beam leads to linewidths which are generally limited by the inverse of the transit time of atoms through the laser beam. Rather than increasing this time by expanding the laser beam diameter (with a consequent loss of intensity), Baklanov *et al.* proposed using two spatially separated beams to obtain structures in the profile of the resonance having a width determined by the time of flight between the two beams. [See also Chebotaev *et al.* (1978).] Similar quantum interference fringes have recently been observed by Bergquist *et al.* (1977) in saturated absorption spectroscopy of a beam of fast neon atoms with spatially separated laser fields. The experiment described below deals with short-lived atomic states (lifetime $\sim 5\times10^{-8}$ sec), so that the transit time through the laser beam ($\sim 10^{-7}$ sec) plays no role in the problem. Consequently, we use two time delayed short pulses instead of two spatially separated beams.[1]

The interference structure appearing in the resonance profile can be simply understood in the following way. Consider first a single pulse of the form $E(t)e^{-i\omega t}$, where the envelope function $E(t)$ has the shape represented in Fig. 2(a) (τ: duration of the pulse). The

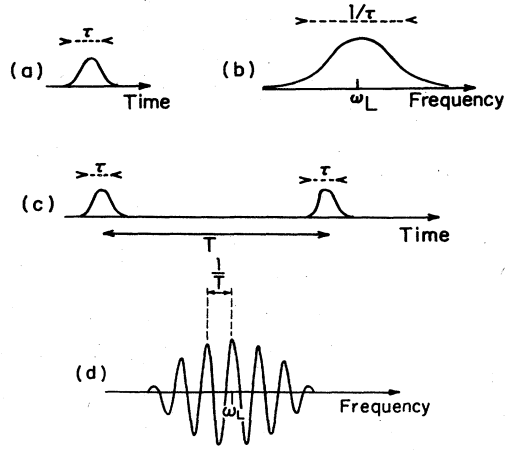

FIG. 2. Single pulse and time-delayed pulses and frequency patterns.

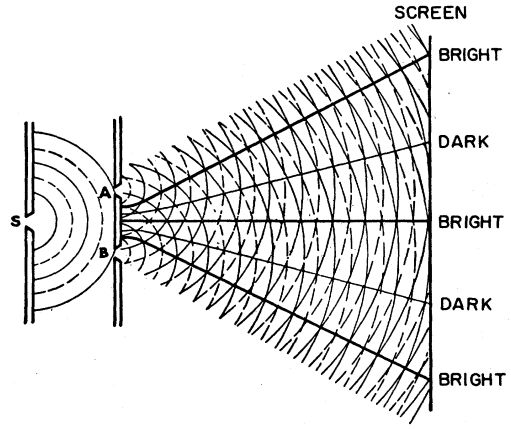

FIG. 3. Wavefronts displaying the two-slit interference modification of the one-slit diffraction pattern.

Fourier analysis of such a pulse leads to a frequency spectrum spread over an interval $1/\tau$ around ω [Fig. 2(b)]. This nonmonochromatic excitation acting upon the atom leads to a Doppler-free two-photon resonance having a width $1/\tau$. Suppose now that $E(t)$ has the shape represented in Fig. 2(c) (two pulses of duration τ separated by a delay T). Just as the diffraction pattern through two spatially separated slits of Fig. 3 exhibits interference fringes within the diffraction profile corresponding to a single slit, the Fourier transform of the electric field corresponding to Fig. 2(c) exhibits interference fringes within the spectrum profile of a single pulse [Fig. 2(d)], with a frequency splitting of $1/T$ between two fringes.

A. Experimental requirements

Two important experimental requirements must be fulfilled in order to obtain such interference fringes in the profile of the two-photon resonance. First, each pusle must be reflected against a mirror placed near the atomic cell in order to expose the atoms to a pulsed standing wave and in this way to suppress any dephasing factor due to the motion of the atoms. As was indicated earlier, the probability amplitude for absorbing two counterpropagating photons is proportional to $e^{i(\omega t-kz)}e^{i(\omega t+kz)}=e^{2i\omega t}$ and does not depend on the spatial position z of the atoms. Second, the phase difference between the two pulses must remain constant during the entire experiment. Significant phase fluctuations between the two pulses will wash out the interference fringes, since any phase variation produces a shift of the whole interference structure within the diffraction background. To avoid such fluctuations, the experiment must be done not with two independent pulses, but with two time-delayed pulses having a constant phase difference during the entire experiment.

B. Theoretical views

From a more physical point of view, one can think of a two-level system, $|g\rangle$ and $|e\rangle$. After the first pulse the atomic state is a coherent superposition of the two levels. Atoms in this superposition freely precess and, depending on the point in time at which the delayed pulse arrives (while the excited atom is still freely precessing), one can see either constructive or destructive interference with the precession of the excited atomic state.

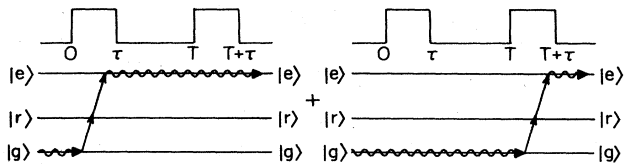

FIG. 4. Two quantum-mechanical amplitudes contributing the total amplitude to order E^2.

Note again that it is important that the initial and the delayed pulses be phase-locked. Otherwise, when the delayed pulse arrives, the random phase difference between initial and delayed pulses will give rise randomly to constructive or destructive interference, and when averaged the interference signal will be washed out.

Yet another interpretation of this interference can be shown diagrammatically:

Figure 4 represents two quantum-mechanical amplitudes whose sum represents the total amplitude, of order E^2 (each photon contributes a factor of E), for reaching the excited state $|e\rangle$ from the ground state $|g\rangle$. The probability of reaching the $|e\rangle$ state is then the absolute square of this sum, and the cross term appearing in this absolute square represents the interference signal.

Higher-order processes can also become important, especially at higher laser intensities. Figure 5 illustrates additional amplitudes of order E^4 which contribute to the interference signal. These diagrams have the physical interpretation of *ac* Stark shift of the $|g\rangle$ and $|e\rangle$ states via mixing with the intermediate state $|r\rangle$. These processes would result in linear power shift of the interference signal.

III. EXPERIMENTAL ARRANGEMENTS

The experiments discussed in this paper were all performed on the 3^2S-4^2D two-photon excitation in sodium. Sodium atoms in the 3^2S ground state were excited to the 4^2D state by two photons at 5787.3 Å (Fig. 6), and the resulting fluorescence at 3302 Å was collected by a photomultiplier. The wavelength of this transition (5787 Å) falls at the peak of the gainband of the rhodamine-6*G* cw (continuous wave) dye laser. Since we wished to employ a cw dye laser oscillator with synchronized pulsed amplifiers in order to obtain a Fourier-limited pulse, this transition was clearly a possible choice for our experiment. One other possible choice

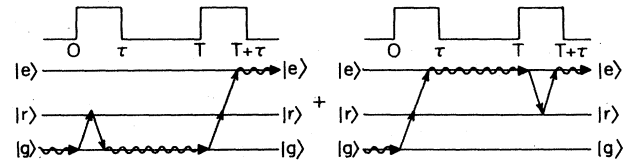

FIG. 5. Two quantum-mechanical amplitudes contributing to the total amplitude to order E^4.

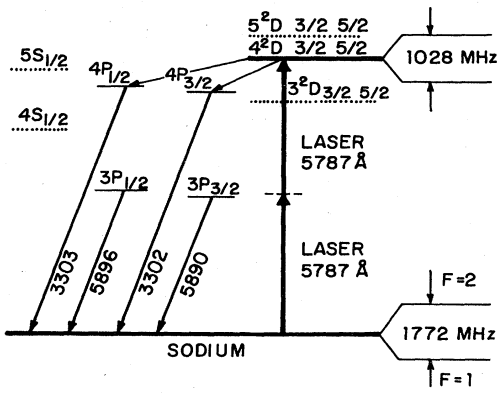

FIG. 6. Energy level diagram of sodium and the two-photon excitation scheme.

was the 3^2S–5^2S two-photon transition, whose wavelength (6022.3 Å) also lies in the gainband of the rhodamine-6G cw dye laser, although with less power (almost a factor of 3 smaller, although various dye mixtures could perhaps substantially increase the gain at 6022 Å). The real advantage of the 3^2S–4^2D transition over the 3^2S–5^2S transition becomes clear, however, when one compares the two-photon transition probabilities for the two transitions. Such comparison (Salour, 1977a) reveals that under normal experimental situations the signal would be 50 times stronger for the 4^2D level than for the 5^2S level. More importantly, since the fine structure of the excited 4^2D state of sodium and the hyperfine structure of the ground state are known very accurately, the 4^2D level would allow a more accurate frequency calibration of our data from the reference sodium cell than the 5^2S level.

A. First approach: Theory

A first possible method for obtaining a sequence of two phase-locked and Fourier-limited pulses is to start with the cw dye laser wave of Fig. 7(a) at frequency ω (having a very long coherence time), and to amplify it with the two time-delayed pulsed amplifiers of Fig. 7(b). Even if the cw lasers delivers a very weak intensity in the spectral range under study, with a sufficient number of synchronized pulsed amplifiers one can obtain enough power to observe the two-photon resonance. The time dependence of the amplified wave has the shape represented by the solid lines of Fig. 7(c). The two pulses are portions of the same sinusoid (represented in dotted lines), and clearly have the same phase, that of the cw carrier wave. Thus if we neglect the cw background, the electric field that excites atoms may be written

$$E(t)=\begin{cases} Ee^{-i(\omega t-\phi)} & \text{for } 0\leq t\leq \tau \\ Ee^{-i(\omega t-\phi)} & \text{for } T\leq t\leq T+\tau \\ 0, & \text{elsewhere,} \end{cases} \tag{1}$$

where

τ is the width of each pulse,

T is the delay between the two pulses,

ω is the cw laser angular frequency, and

ϕ is the phase of the cw laser carrier.

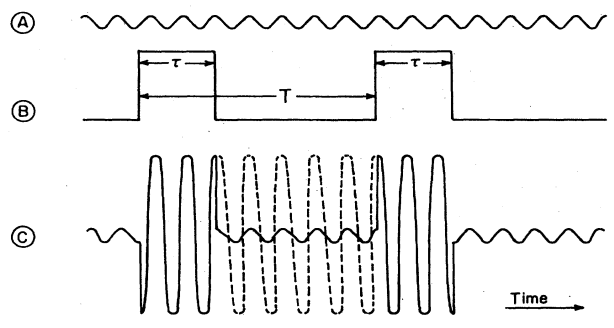

FIG. 7. Pulsed amplification of cw dye laser wave: (a) cw laser wave; (b) Time dependence of amplification; (c) Amplified wave.

The theoretical treatment of coherent effects associated with the two-photon resonance has been presented in several different formalisms. (See, for example, Takatsuji, 1971, 1975; Brewer and Hahn, 1975; Hartmann, 1968; Belenov and Poluektov, 1969; Bassini *et al.*, 1977; Li, 1977; and Weingarten, 1972.) Grischkowsky *et al.* (1975) have introduced a two-photon vector model which assumes that the light is applied adiabatically with respect to the single-photon transitions to the intermediate states. While, in general, two-photon coherent effects are more complicated than one-photon effects, and single-photon processes such as photon echoes (Abella *et al.*, 1964, 1966), optical nutation (Hocker and Tang, 1968, 1969), adiabatic following (Grischkowsky, 1970) and adiabatic double passage (Treacy, 1968; Treacy and DeMaria, 1969; Loy, 1974) clearly have their two-photon analogs, one can also look for two-photon effects that have no one-photon analogs (Grischkowsky *et al.*, 1975). It is shown, however, (Salour, 1977a) that the two-photon transition between the ground state $|g\rangle$ and the excited state $|e\rangle$ induced by two counterpropagating waves of amplitude E and frequency ω, for a separation of $\omega_0=2\omega$, is equivalent to the problem of a two-level system $|1\rangle$ and $|2\rangle$, separated by ω_0 (where ω_0 is the Bohr frequency of the atomic transition), with an "effective" dipole moment $\mathfrak{D}$, excited by a field $\mathcal{E}e^{-i(2\omega t-\theta)}$, where $\mathcal{E}$ is proportional to E^2, θ is a phase depending on the mirror reflecting the incident wave, and $\mathfrak{D}$ is proportional to $\sum_r\langle e|\mathbf{D}|r\rangle\langle r|\mathbf{D}|g\rangle/(E_g+\omega-E_r)$, where $\mathbf{D}$ is the atomic dipole moment. (To simplify calculations, we take $\hbar=1$ throughout this paper.)

Again we note that in calculating the probability amplitude for absorbing two counterpropagating photons, the two $\mathbf{r}$-dependent factors ($e^{i\mathbf{k}\cdot\mathbf{r}}$ and $e^{-i\mathbf{k}\cdot\mathbf{r}}$) cancel when multiplied. Hence the position $\mathbf{r}$ of the atom plays no role in our problem, and the motion of the atoms causes no dephasing.

Using the Schrödinger equation for this two-level system,

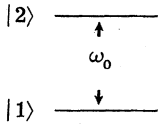

$$|\psi\rangle=a(t)|1\rangle+b(t)|2\rangle, \tag{2}$$

one finds the equation for the evolution of b

$$i\dot{b} = \omega_0 b - \mathfrak{D}\mathcal{E}(t)a . \tag{3}$$

From the incident wave of Fig. 7(c), we can determine the value of $\mathfrak{D}\mathcal{E}(t)$ to be

$$-\mathfrak{D}\mathcal{E}(t) = \begin{cases} \omega_1 e^{-2i\omega t} & \text{for } 0 \leq t \leq \tau \\ \omega_1 e^{-2i\omega t} & \text{for } T \leq t \leq T+\tau , \\ 0 & \text{elsewhere} \end{cases} \tag{4}$$

where

$$\omega_1 \sim E^2 . \tag{5}$$

Note that the phases ϕ [appearing in Eq. (1)] and θ (appearing in $e^{-i(2\omega t-\theta)}$) disappear at the end of our calculations, and thus can be taken as equal to zero from the beginning.

We can simplify our calculation by going to the interaction representation, taking:

$$\begin{cases} \tilde{a} = a \\ \tilde{b} = be^{i\omega_0 t} \end{cases} . \tag{6}$$

Thus from Eqs. (4) and (5) the Schrödinger equation becomes:

$$\begin{cases} i\dot{\tilde{b}} = \omega_1 e^{i(\omega_0 - 2\omega)t}\,\tilde{a} & \text{for } 0 \leq t < \tau \text{ and for } T \leq t \leq T+\tau \\ i\dot{\tilde{b}} = 0 & \text{elsewhere} \end{cases} . \tag{7}$$

For the two-photon process we can assume that ω_1 is sufficiently small, and that the duration τ of each pulse is sufficiently short, so that if atoms are in the lower state before the first pulse (i.e., $a=1$ and $b=0$), then $\tilde{b}(t)$ remains very small after each pulse, and $\tilde{a}(t)$ is practically equal to 1. Consequently, we can replace $\tilde{a}$ by one in Eq. (7) and thus obtain

$$\begin{cases} i\dot{\tilde{b}} = \omega_1 e^{i(\omega_0 - 2\omega)t} & \text{for } 0 \leq t \leq \tau \text{ and for } T \leq t \leq T+\tau \\ i\dot{\tilde{b}} = 0 & \text{elsewhere} \end{cases} . \tag{8}$$

It is possible to perform the calculations for any value of ω_1 and τ by using the rotating frame representation rather than the interaction representation, of course. But the perturbative calculation presented here is much simpler and contains the main physical ideas.

In order to find the state of the atom after the first pulse, we integrate Eq. (8) between zero and τ with the initial condition $\tilde{b}(0)=0$. We obtain the probability amplitude $b_1 = \tilde{b}(\tau)$ for finding the atom in the upper state immediately after the first pulse

$$b_1 = \tilde{b}(\tau) = -\frac{\omega_1}{\omega_0 - 2\omega}\left[e^{i(\omega_0 - 2\omega)t} - 1\right]. \tag{9}$$

Note that according to Eq. (8), $\tilde{b}(t)$ does not change between the two pulses, but remains equal to b_1. (For the time being we have neglected the damping due to spontaneous emission. We will take it into account later.) Therefore, by integrating Eq. (8) between T and $T+\tau$ with the initial condition $\tilde{b}(T) = b_1$, we obtain the probability amplitude $b_2 = \tilde{b}(T+\tau)$ for finding the atom in the upper state after the second pulse

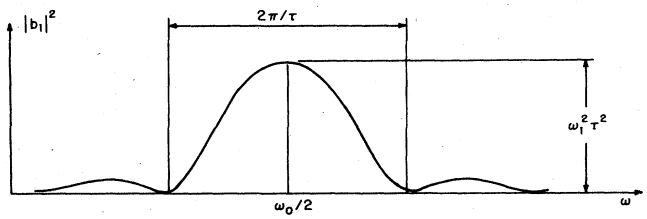

FIG. 8. $|b_1|^2$ as a function of the laser angular frequency ω.

$$b_2 - b_1 = -\frac{\omega_1}{\omega_0 - 2\omega}\left[e^{i(\omega_0 - 2\omega)(T+\tau)} - e^{i(\omega_0 - 2\omega)T}\right]$$
$$= b_1 e^{i(\omega_0 - 2\omega)T} . \tag{10}$$

Thus we find

$$b_2 = b_1\left[1 + e^{i(\omega_0 - 2\omega)T}\right]. \tag{11}$$

Since we neglect the damping due to spontaneous emission, $\tilde{b}(t)$ remains equal to b_2 for $t \geq T+\tau$. From the experimental point of view, if the photomultiplier detecting the fluorescence is gated so that it opens only for $t \geq T+\tau$, the detected signal then is proportional to $|b_2|^2$.

From Eq. (9) we obtain:

$$|b_1|^2 = \omega_1^2\left[\frac{\sin(\omega_0 - 2\omega)\tau/2}{(\omega_0 - 2\omega)/2}\right]^2 , \tag{12}$$

where $|b_1|^2$ is the probability of excitation of the atom after the first pulse. Figure (8) shows the plot of $|b_1|^2$ as a function of the laser's angular frequency ω. It is a diffraction curve centered at $\omega = \omega_0/2$ with a width of the order of $2\pi/\tau$, i.e., inversely proportional to the duration τ of a single pulse.

From Eq. (11), however, we obtain

$$|b_2|^2 = |b_1|^2\,|1 + e^{i(\omega_0 - 2\omega)T}|^2$$
$$= 4|b_1|^2\left[\cos\frac{\omega_0 - 2\omega}{2}\,T\right]^2 . \tag{13}$$

The oscillatory term in Eq. (13) corresponds to interference fringes appearing within the diffraction profile $4|b_1|^2$. Figure 9 shows the plot of $|b_2|^2$ as a function of ω. The fringe spacing $\Delta\omega$ is given by the period in ω of the $[\cos(\omega_0 - 2\omega)/2T]^2$ term of Eq. (13)

$$\Delta\omega = \pi/T . \tag{14}$$

Since $\omega = 2\pi\nu$, the fringe spacing is

$$\Delta\nu = 1/2T . \tag{15}$$

Substituting $|b_1|^2$ from Eq. (12) into Eq. (13), we obtain

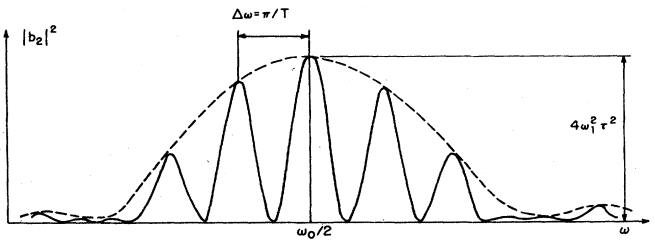

FIG. 9. $|b_2|^2$ as a function of the laser angular frequency ω.

$$|b_2|^2 = 4\omega_1^2\tau^2\left[\frac{\sin(\omega_0-2\omega)\tau/2}{(\omega_0-2\omega)\tau/2}\right]^2\left[\cos\frac{\omega_0-2\omega}{2}\,T\right]^2. \tag{16}$$

Thus $|b_2|^2$ has its maximum value when $\omega=\omega_0/2$. Consequently, if we neglect the light shifts, the central fringe is *exactly centered* at $\omega=\omega_0/2$. Furthermore, the position of the central fringe does not depend on T, while the spacing between fringes is T dependent. T can fluctuate for various reasons, such as instability or vibration in the optical delay line; however, any fluctuations in T will not affect the position and amplitude of the central fringe, but will rather produce a decrease in the amplitude of the lateral fringes. Experiments can be performed either by varying ω, with ω_0 and T held fixed, or by varying the Bohr frequency of atomic transition ω_0 (for example, by Zeeman tuning), holding ω and T fixed. Note that, since the central fringe is always exactly centered, small fluctuations of T are not crucial for experiments of this type, as far as spectroscopic applications are concerned. Note also that ω and ω_0 play a symmetric role in our experiment. Of course, one can also vary T, with ω_0 and ω held fixed; such a procedure is discussed later.

Thus far, we have neglected the decay of the excited state populations due to spontaneous emission. This is a good approximation when the delay time T between the two pulses is much less than the radiative lifetime of the excited state, i.e., pulse duration $\tau < T \ll$ radiative lifetime $\tau_R = 1/\Gamma$, where Γ is the natural linewidth of the excited state.

However, when T is not shorter than the radiative lifetime of the excited state, one needs to take into account the decay of b_1 by a factor of $e^{-\Gamma T/2}$ between the first and the second phase-locked pusles. Thus one should replace b_1 by $b_1 e^{-\Gamma T/2}$ in the left-hand side of Eq. (10)

$$b_2 - b_1 e^{-\Gamma T/2} = b_1 e^{i(\omega_0-2\omega_0)T} \tag{17}$$

or

$$b_2 = b_1\left[e^{-\Gamma T/2} + e^{i(\omega_0-2\omega)T}\right]. \tag{18}$$

The two terms which interfere in the bracket of Eq. (18) no longer have the same modulus, and the contrast of the interference fringes is thus no longer equal to one. When the interference of these two terms is maximum, the square of this bracket takes the value $[1+e^{-\Gamma T/2}]^2$. The minimum value, on the other hand, is equal to $[1-e^{-\Gamma T/2}]^2$. Thus the contrast of the fringes is

$$c = \frac{(1+e^{-\Gamma T/2})^2-(1-e^{-\Gamma T/2})^2}{(1+e^{-\Gamma T/2})^2+(1-e^{-\Gamma T/2})^2} = \frac{2e^{-\Gamma T/2}}{1+e^{-\Gamma T}}. \tag{19}$$

Hence the contrast, which is equal to one for $T \ll 1/\Gamma$, tends to 0 when $T \gg 1/\Gamma$. Also note that when $T = 1/\Gamma = \tau_R$, then $c \simeq 0.5$. In other words, increasing the delay between the two pulses causes the fringe spacing and the fringe contrast to decrease; consequently, one obtains better resolution with a smaller signal-to-noise ratio. This can be understood by noting that when $T > \tau_R$, a smaller number of atoms can live for a sufficiently long time to experience the second pulse; since it is interference due to the second pulse that provides the high resolution, only the still-excited atoms contribute to the signal.

Note that in this type of experiment any jitter in cw dye laser frequency will also contribute to a reduction in contrast. For this reason, the laser used in our experiment was frequency stabilized to a pressure-tuned reference etalon.

B. First approach: Setup and results

Figure 10 shows our experimental setup. We utilized a single mode cw dye laser (Spectra Physics 580A, fre-

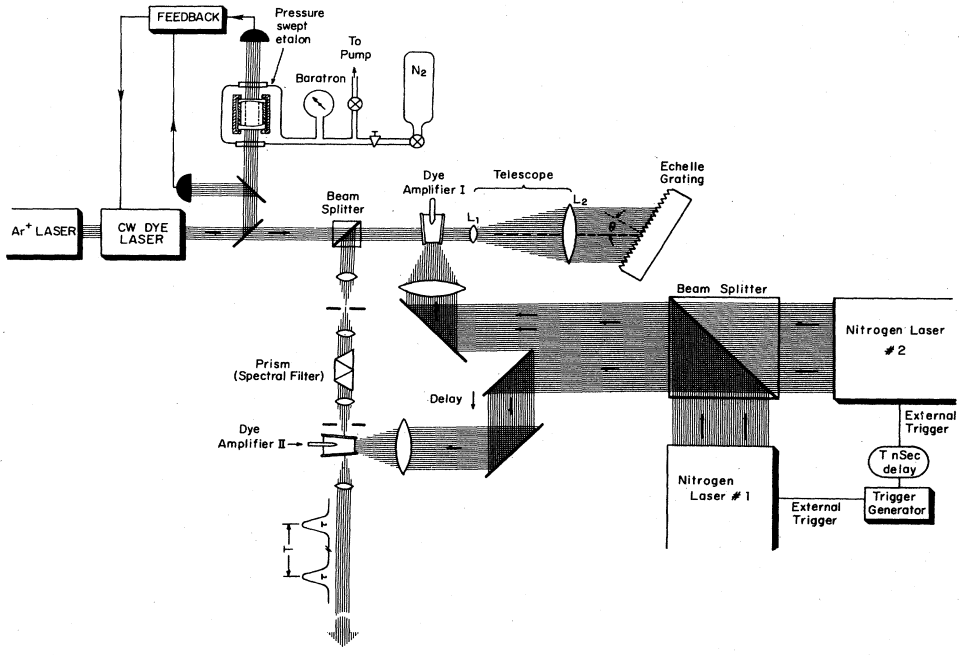

FIG. 10. The experimental arrangement.

quency-stabilized to a pressure-tuned reference etalon and pumped by a Spectra Physics 164 Ar^+ laser) which was tuned to the 3^2S-4^2D two-photon transition in sodium at 5787.3 Å. The output of this cw dye laser (40 mW, 2MHz) was then amplified in two synchronized stages of dye amplifiers, first in a double-pass amplifying dye cell (I) and then in a single-pass dye amplifier (II), pumped by two externally triggered, synchronized, time-delayed nitrogen lasers. The construction of this oscillator-amplifier system, when pumped by only one nitrogen laser, is discussed in detail elsewhere (Salour, 1977c).

The two nitrogen lasers (one a Molectron uv-1000, the other a home-built N_2 laser, both having a pulse width of 8 nsec) were externally triggered by a home-built trigger generator in such a way that the second nitrogen laser was triggered a time T (several nanoseconds) after the first. The outputs of the nitrogen lasers were mixed in a beam splitter cube which was coated for 50% reflection at 3371 Å at a 45° angle of incidence. Great care was taken that the output of the N_2 lasers would be completely collinear after passing through the beam splitter cube, and the intensity of the uv-1000 N_2 laser was adjusted so that after passing through the beam splitter cube the intensities of both collinear outputs were equal. This collinear output of the beam splitter was equally distributed (by mirrors of very high reflectivity at 3371 Å) between the two amplifying dye cells in such a way that the pump light for the dye amplifier II would arrive slightly later than the input from the evolving pulses building up from the double-pass dye amplifying cell (I).

The output of dye amplifier II consisted of two time-delayed pulses of 4 nsec duration and 60 kW power at 10 pulses/sec. This output was sent into a sodium cell (Fig. 11) which was kept at 130°C (2×10^{-6} Torr of vapor pressure). The sodium cell was made of Corning 1720 calcium alumino-silicate glass with optically flat windows and was baked at high temperature and later filled with sodium under very high vacuum to avoid any foreign gas contamination. A highly reflective mirror of 2-m radius of curvature was placed very close to the other window of the sodium cell in order to generate the laser standing waves. The output of the photomultiplier (EMI 9635 QB) monitoring the fluorescence from $4P$ to $3S$ at 3303 Å was processed by a boxcar integrator, and the result was recorded by a chart recorder.

After very many unsuccessful attempts to observe interference fringes, it became clear that although theoretically the two pulses should have been locked in phase to the phase of the cw carrier, experimentally they were not. One possible explanation for the absence of interference fringes can be linked to the Kramers–Kronig argument that the time-pulsed amplification is intrinsically accompanied by a time-pulsed refractive index. This index of refraction variation from one pulse to the other would give rise to a random phase difference between the two pulses and the cw carrier wave, which when averaged would wash out the interference fringes.

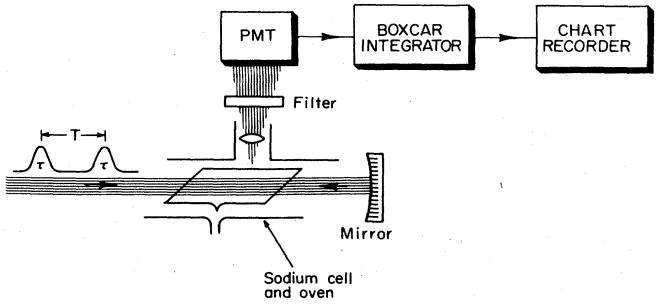

FIG. 11. Experimental sodium cell and analysis arrangement.

C. Second approach: Theory

A second possible method of generating a sequence of two phase-locked and Fourier-limited pulses is to start with a Fourier-limited pulse (obtained by amplifying a cw wave) and to generate two pulses from it in an optical delay line (Salour, 1976a; Salour and Cohen-Tannoudji, 1977). The time dependence of the resulting wave has the shape represented by the solid lines of Fig. 12. The second pulse is just the time translation of the first one by an amount T, $(T>\tau)$. However, the sinusoid extrapolated from the first pulse (dotted lines) generally does not match the second pulse, which means that the two pulses do not have the same phase, unless T is an integral multiple of the optical period $2\pi/2\omega$ (i.e., $e^{i\omega T}=\pm1$). The phase shift appearing in Fig. 12 depends on T, and thus T must remain constant with a good precision, which requires a very stable optical delay line. This situation contrasts with the experiments of Fig. 7, where the fluctuations of T were not critical.

One can write the electric field corresponding to the two pulses of Fig. 12

$$E(t)=\begin{cases} E\,e^{-i(\omega t-\phi)} & \text{for } 0\le t\le\tau \\ Ee^{-i[\omega(t-T)-\phi]} & \text{for } T\le t\le T+\tau \\ 0 & \text{elsewhere}\end{cases}. \tag{20}$$

Thus the corresponding $\mathfrak{D}\mathcal{E}(t)$ is

$$-\mathfrak{D}\mathcal{E}(t)=\begin{cases} \omega_1 e^{-2i\omega t} & \text{for } 0\le t\le\tau \\ \omega_1 e^{-2i\omega(t-T)} & \text{for } T\le t\le T+\tau \\ 0 & \text{elsewhere}\end{cases}, \tag{21}$$

where

$$\omega_1\sim E^2 .$$

Note that for $0\le t\le\tau$, Eqs. (21) and (4) are identical. Thus, after integrating the Schrödinger equation, the value of b_1 will be the same as that of Eq. (9). On the other hand, the value of b_2 is obtained by integrating:

$$i\dot{\tilde{b}}=\omega_1 e^{i\omega_0 t}e^{-2i\omega(t-T)}=\omega_1 e^{i(\omega_0-2\omega)t}e^{2i\omega T} \tag{22}$$

between T and $T+\tau$, with the initial condition $\tilde{b}(T)=b_1$;

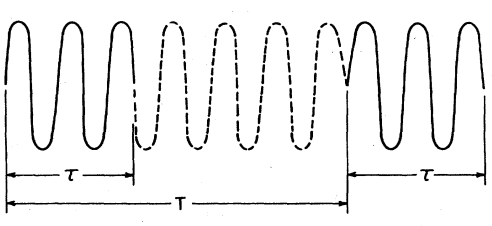

FIG. 12. Pulse pair generated by an optical delay line. Note the difference in phase.

thus one obtains

$$b_2 - b_1 = b_1 e^{i(\omega_0 - 2\omega)T} e^{2i\omega T} = b_1 e^{i\omega_0 T}, \tag{23}$$

or

$$b_2 = b_1[1 + e^{i\omega_0 T}]. \tag{24}$$

Therefore

$$|b_2|^2 = 4|b_1|^2 \cos^2(\omega_0 T/2). \tag{25}$$

Thus one obtains interference fringes within the diffraction profile centered at $\omega_0 = 2\omega$, associated with $|b_1|^2$, with a period

$$\Delta\omega_0 = 2\pi/T. \tag{26}$$

Note that in general the central fringe is not centered at $\omega_0 = 2\omega$. Figure 13 shows the variation of $|b_2|^2$ as a function of ω_0, with ω and T held fixed. The dotted line corresponds to the diffraction profile of $|b_1|^2$.

Note that from Eqs. (25) and (12) we have

$$|b_2|^2 = 4\omega_1^2 \left[\frac{\sin(\omega_0 - 2\omega)\tau/2}{(\omega_0 - 2\omega)/2}\right]^2 \cos^2 \frac{\omega_0 T}{2}$$

$$= 4|b_1|^2 \cos^2 \frac{\omega_0 T}{2}. \tag{27}$$

Therefore the only variation of $|b_2|^2$ with ω comes from $|b_1|^2$, i.e., from the diffraction profile. Thus if ω is varied, with ω_0 and T held fixed, one does not expect any interference fringes. The difficulty is that when ω varies, the second pulse is dephased by an amount $e^{i\omega T}$ with respect to the first pulse (see Fig. 12); thus when ω is averaged, the interference fringes will be washed out.

One possible scheme for locking the phases of the two pulses, and consequently causing the interference fringes to reappear, centered exactly at $\omega = \omega_0/2$, is to simultaneously vary T when ω is varied in such a way that $e^{i\omega T} = \pm 1$. Then $e^{2i\omega T}$, the dephasing factor between the two effective fields for the two-photon resonances in Eq. (22), becomes $[e^{i\omega T}]^2 = [\pm 1]^2 = 1$.

The fact that T varies simultaneously with ω is not important for this experiment, since, as we showed in the description of the experiment of Fig. 7, when the two pulses of effective electric field are in phase the central fringe is exactly centered, and small variations of T do not affect it as long as $e^{2i\omega T}$ remains equal to +1.

Furthermore, since we set $\Delta\phi = \nu\Delta T + T\Delta\nu = 0$, so that $\Delta\nu/\nu = -\Delta T/T$ is small (since $\Delta\nu$ is of the order of $1/\tau$ ~ 50 MHz $\ll \nu$), the fringe splitting is practically unaffected.

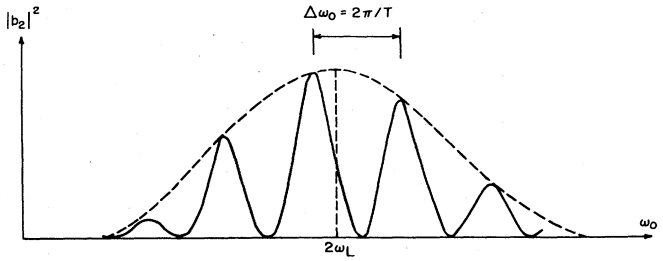

FIG. 13. $|b_2|^2$ as a function of Bohr angular frequency ω_0 of atomic transition.

We will describe later how we vary T simultaneously with ω in order to keep $e^{i\omega T} = \pm 1$ in our experiment.

D. Second approach: Setup and results

Figure 14 shows the experimental arrangement (Salour, 1976a; Salour and Cohen-Tannoudji, 1977). We utilized a single mode cw dye laser (Spectra Physics 580A, frequency-stabilized to a pressure-tuned reference etalon, and pumped by a Spectra Physics 165 Ar^+ laser) which was tuned to the 3^2S–4^2D two-photon transition in sodium (5787.3 Å). (Note: the lifetime of the 4^2D state is $\sim 5\times10^{-8}$ sec.) The output of this cw dye laser (40 mW, 2MHz) was then amplified in three synchronized stages of dye amplifiers pumped by a 1 MW nitrogen laser. (Three stages of amplification were necessary to boost the peak output power to an acceptable level for this experiment.) The pump light for the amplifiers was geometrically divided between the amplifiers, and was optically delayed in order to arrive slightly later than the input from the evolving pulse building up from the cw dye laser, to maximize the length of the output pulse. To avoid undesirable amplified spontaneous emission from the amplifiers, suitable spectral and spatial filters were inserted between stages. [A detailed description of this oscillator-amplifier dye laser system is presented in Salour (1977c).] The 75 kW output of the third-stage amplifier was split into two parts, one of which went into a reference sodium cell, and one of which was further split into another two parts. The first of these (part A in Fig. 14) was sent directly into a

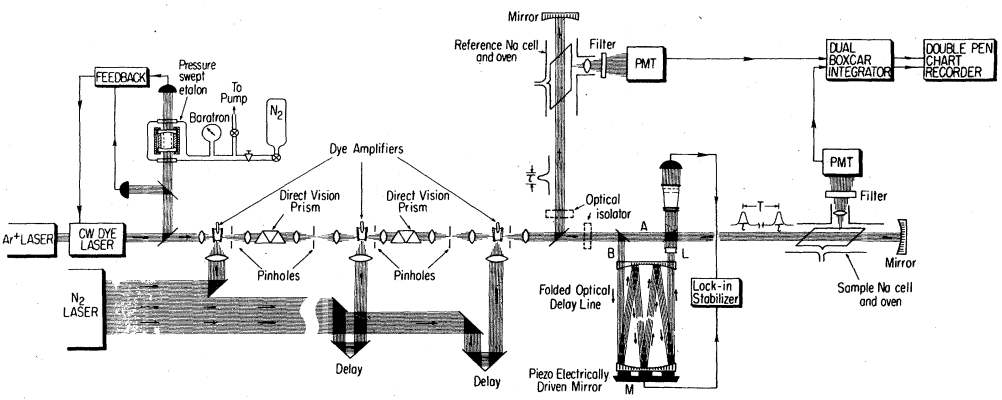

FIG. 14. The experimental arrangement.

sample sodium cell, and the second (part B in Fig. 14) was optically delayed in a delay line by a time T ($2T = 18, 25, 33$ nanoseconds), and subsequently recombined with the first and focused into the sample sodium cell. We stabilized the delay line by locking the center fringe of the two cw carrier beams (which is at maximum when the direct and the delayed cw carrier beams are in phase, i.e., when $e^{i\omega T} = 1$) to the motion of the mirror M, which was mounted on a piezoelectric ceramic. In this way, the two time-delayed and Fourier-limited pulses were phase-locked during the entire experiment. Furthermore, the delayed beam, with its longer optical path, had wavefronts with a larger radius of curvature than those of the direct beam, so a high quality lens (L) was used to match the curvature of the two wavefronts. Both sodium cells were kept at 130°C (2×10^{-6} Torr of vapor pressure); they were made of Corning 1720 calcium alumino-silicate glass with optically flat windows and were baked at high temperature and later filled with sodium under very high vacuum to avoid any foreign gas contamination. To generate the laser standing waves with short pulses, the back-reflecting mirror was adjusted so that the time delay between the original pulse and the back-reflected pulse was significantly shorter than the pulse duration τ. The outputs of the two photomultipliers (EMI 9635 QB) monitoring the fluorescence from $4P$ to $3S$ at 3303 Å were simultaneously processed by a dual channel boxcar integrator, whose 100-nsec-wide gates were independently triggered after the delayed pulse (for the sample cell) and after the original pulse (for the reference cell). The results were recorded simultaneously by a dual pen chart recorder.

Figures 15, 16, and 17 show typical traces obtained for delays with $2T = 18$, 25, and 33 nsec, respectively, between the two pulses. The upper portion of each trace corresponds to the four well-known two-photon resonances of the 3^2S–4^2D transition of sodium observed in the reference cell with a single pulse, while the lower portion of each trace corresponds to the same four resonances observed in the sample cell which is excited by the two time-delayed coherent pulses. An interference structure clearly appears on each resonance in the lower portion of each trace. Figure 18 shows a plot of the splitting between the fringes as a function of T_{eff}^{-1}, where $T_{\text{eff}} = 2T$ is the effective delay time between the two phase-locked pulses. The error bars are due largely to

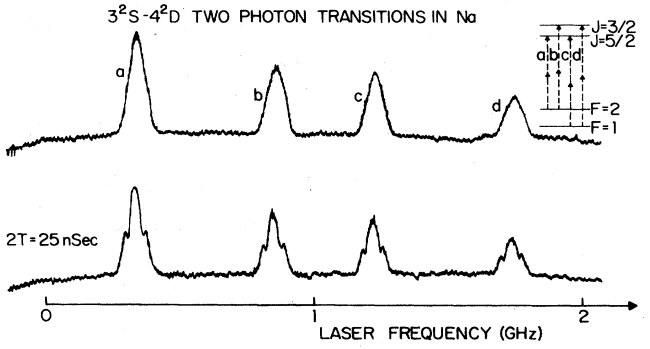

FIG. 16. Typical experimental traces for a delay of 25 nsec.

statistical errors and to the precision involved in measuring the exact fringe splittings, which were calibrated by the known fine structure of the 4^2D excited state and hyperfine structure of the 3^2S ground state in the upper trace. It was also verified that, with the delay line unlocked, the interference fringes, as ω varied, disappeared.

Clearly, it is possible to choose T longer than the radiative lifetime of the excited state, in which case the resolution would be better than the natural linewidth. In such a case, however, only those atoms that remain in the excited state for a time at least equal to T would contribute to the interference effect, and consequently the fringes would have a very poor contrast. This is verified in the bottom traces of Figs. 15, 16, and 17 which show that the contrast of the fringes becomes progressively smaller when longer delay is used. This can be understood analytically from the influence of the radiative lifetime of the excited states [Eq. (19)], since by increasing T one obtains a better resolution (i.e., fringe spacing decreases) accompanied by a smaller contrast, and consequently a smaller signal-to-noise ratio.

IV. ISOLATION OF FRINGES

A. Theory

When the contrast is not equal to one, it is possible to eliminate the diffraction background in order to isolate the interference fringes (Salour, 1977b). One can introduce a phase shift on the second pulse of Fig. 2(c) by, for example, sending the two pulses through a crystal plate and applying an electric field to the plate im-

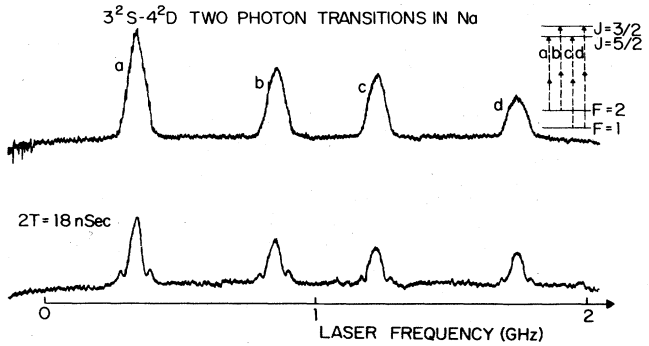

FIG. 15. Typical experimental traces for a delay of 18 nsec.

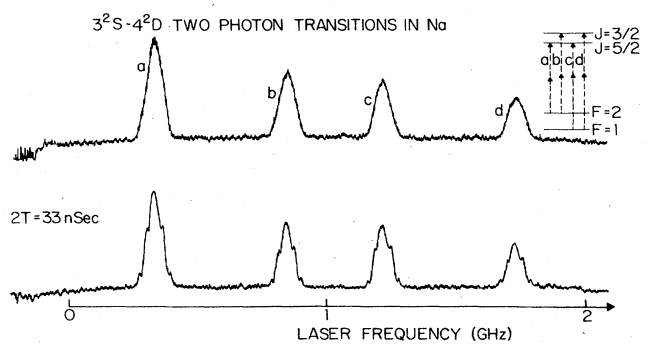

FIG. 17. Typical experimental traces for a delay of 33 nsec.

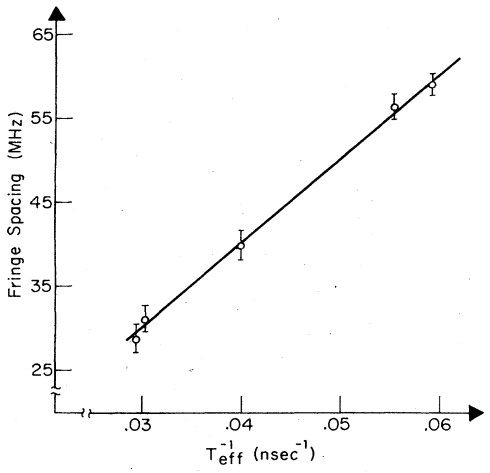

FIG. 18. Splitting between the fringes as a function of T_{eff}^{-1}.

mediately after the first pulse has passed through, so that the index of refraction changes *for the second pulse only*. If $e^{i\delta}$ is the phase shift for the second pulse, then Eq. (4) will become:

$$-\mathfrak{D}\mathcal{E}(t)=\begin{cases}\omega_1 e^{-2i\omega t} & \text{for } 0\leq t\leq\tau\\ \omega_1 e^{-2i(\omega t-\delta)} & \text{for } T\leq t\leq T+\tau\\ 0 & \text{elsewhere}\end{cases}, \tag{4'}$$

where

$$\omega_1 \sim E^2 . \tag{5'}$$

Note that in Eq. (9), b_1 does not change, but $b_2 - b_1$ is multiplied by $e^{2i\delta}$ in Eq. (10), so that Eq. (11) becomes

$$b_2 = b_1[1+e^{i[(\omega_0-2\omega)T+2\delta]}].$$

Note also that ω and T are locked together so that $e^{i\omega T}=\pm 1$; hence Eqs. (11) and (24) are equivalent, and the former shows the structure more clearly. Thus

$$|b_2|^2 = 4|b_1|^2\left[\cos\frac{(\omega_0-2\omega)T+2\delta}{2}\right]^2 . \tag{28}$$

This produces a shift δ/T of the whole interference structure within the diffraction profile. If δ is chosen equal to $\pi/2$ (by applying the proper voltage to the crystal), then the shift corresponds to half of a fringe spacing By subtracting the signals corresponding to $\delta=0$ and $\delta=\pi/2$, one obtains

$$\begin{aligned}|b_2(\delta=0)|^2 - \left|b_2\left(\delta=\frac{\pi}{2}\right)\right|^2 &= 4|b_1|^2\left[\cos^2\frac{(\omega_0-2\omega)T}{2}-\sin^2\frac{(\omega_0-2\omega)T}{2}\right]\\ &= 4|b_1|^2\left[2\cos^2\frac{(\omega_0-2\omega)T}{2}-1\right].\end{aligned} \tag{29}$$

Thus not only is the diffraction background suppressed, but the interference signal is automatically doubled. Note that it remains centered at $\omega=\omega_0/2$.

B. Setup and results

Figure 19 shows our experimental setup. It is identical to the arrangement of Fig. 14, except that the N_2 laser was externally triggered by a homemade trigger generator. The trigger generator produced a train of pulses. For simplicity, let us distinguish between the first and the second pulses by calling the first pulse A and the second pulse B. Thus the train of pulses from the trigger generator consisted of a train of A, B pulses. (A and B pulses were each 8 nsec long, 50 msec apart.)

While a train of A, B pulses triggered the N_2 laser, a flip-flop counter discriminated A pulses from B pulses, and after a proper delay the A pulses triggered boxcar I, and the B pulses triggered boxcar II. Since each A pulse and each B pulse from the dye laser gave rise to a pair of A and a pair of B pulses at the sodium sample cell, the electronic delay was adjusted so that the 100-nsec-wide gates of both boxcars were opened immedi-

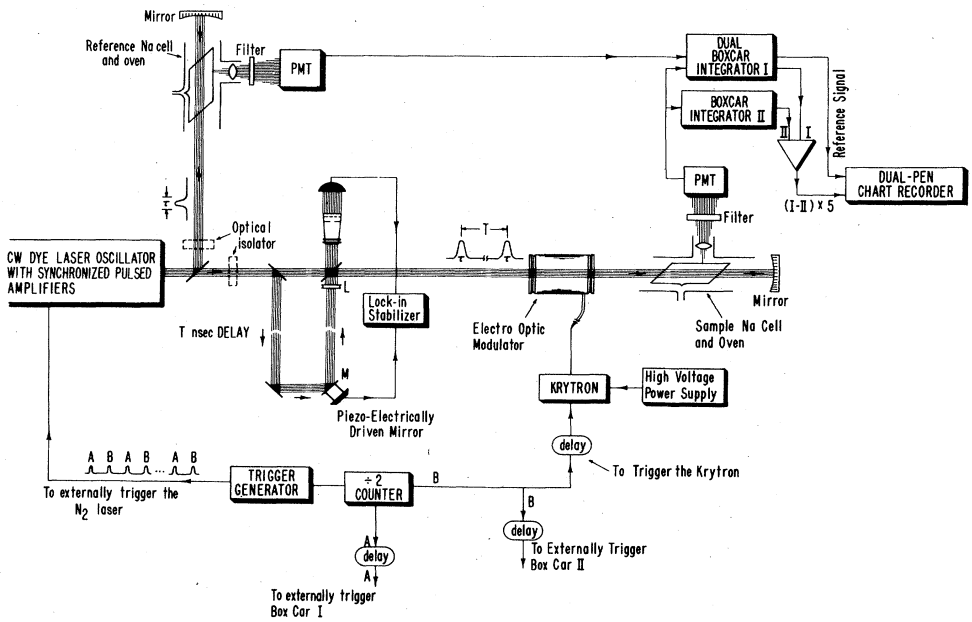

FIG. 19. The experimental arrangement.

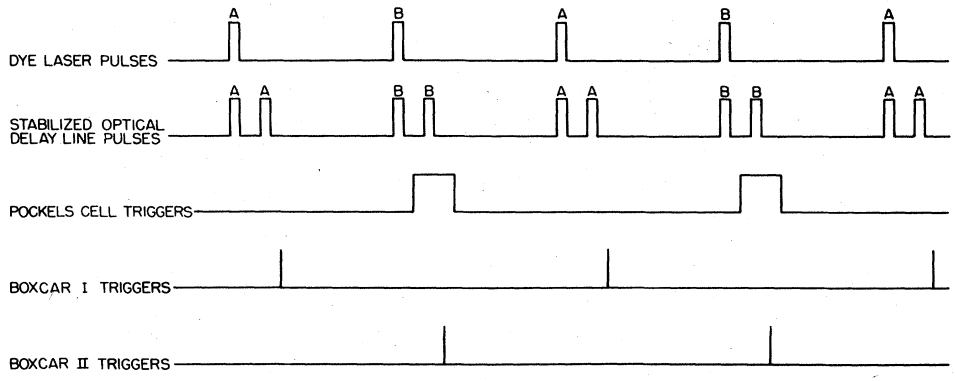

FIG. 20. Timing of trigger signals.

ately after the delayed pulses, as illustrated in Fig. 20. Meanwhile, the B pulses triggered an EG&G KN-22 Krytron switch which turned on a Pockels cell (Interactive Radiation Model 212-080, or Isomet Model EON4203). The voltage on the Pockels cell was adjusted so that it would produce a 90° phase shift on the delayed B pulses; moreover, the Krytron switch turned on slightly ahead of the delayed B pulses and turned off slightly after the delayed B pulses, as illustrated in Fig. 20. For this reason, proper care had to be taken in the design of the trigger generator so that the Pockels cell remained on before and after the delayed B pulses to allow for any possible jitter associated with the rise time of the KN-22 Krystron and the Pockels cell. The outputs of the two boxcar integrators were subtracted in a linear differential amplifier and the result was recorded on a chart recorder.

The reference sodium cell used in our experiment allowed us not only to calibrate the frequency accurately (since the cw oscillator was frequency stabilized to a pressure-tuned reference etalon), but also to examine the elimination of the diffraction background as a result of the 90° phase shift between B pulses. The output of the reference PMT (EMI-9635 QB) monitoring the resulting $4P \rightarrow 3S$ fluorescence at 3302 Å due to single pulse excitation (train of A, B pulses) was processed by the other channel of the PAR 162 boxcar integrator, whose gate was triggered just after the A and B pulses, and the resulting fluorescence was recorded by the same dual pen chart recorder.

Figure 21 shows the experimental results for a delay of 25 nsec. The upper trace corresponds to the reference sodium cell. A number of important tests were performed to assure that these data corresponded to real isolated Ramsey fringes. First, it was verified that no signal was observed when zero phase shift was introduced between B pulses (by turning off the high voltage supply to the Krystron). Figure 22 shows this result; the upper trace corresponds to the reference cell, and the lower trace corresponds to the sample cell when zero phase shift was introduced between B pulses. (An equivalent test would have been to induce a 180° phase shift between B pulses, in which case one again expects a null signal. However, the electronic circuitry for triggering the Krytron did not allow us to increase the voltage enough to provide a 180° phase shift. A slight modification in the electronic design should make this test also possible.) Second, by slightly varying the voltage supplied to the electro-optic modulator, and thus in effect slightly varying the phase of the phase-shifted delayed B pulses, the signal was optimized, so that at the voltage corresponding to the exact 90° phase shift the diffraction background was completely eliminated. There was still some small background in some of the experimental traces which could be eliminated only by making a slight adjustment in the Krytron power supply voltage. This was attributed to the induced phase jitter associated with the electro-optic modulator; the pulse-to-pulse jitter in the phase shift induced by the Pockels cell may have been the source of this difficulty.

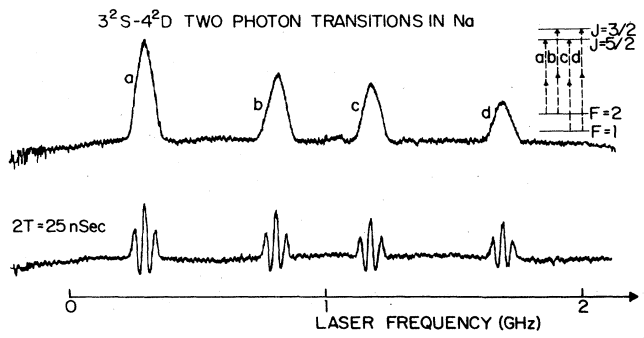

FIG. 21. Typical experimental traces for a delay of 25 nsec with 90° phase modulation between alternate delayed pulses.

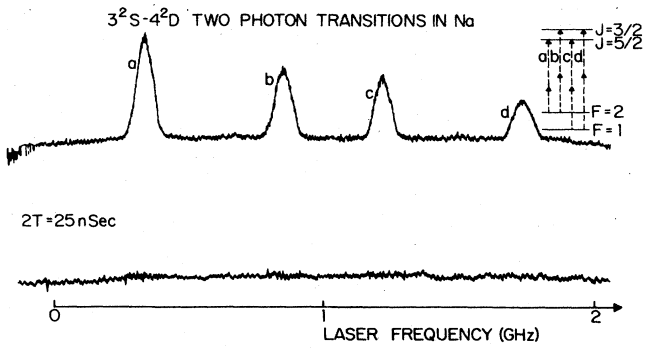

FIG. 22. Typical experimental traces for a delay of 25 nsec with zero phase modulation between alternate delayed pulses.

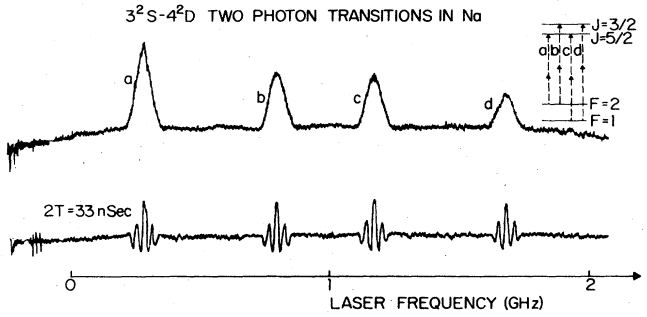

FIG. 23. Typical experimental trace for a delay of 33 nsec with 90° phase modulation between alternate delayed pulses.

Figure 23 shows similar experimental results for a delay of 33 nsec. Again the upper trace corresponds to the reference cell, and the lower trace corresponds to the isolated Ramsey fringes. Note that in this case the fringe spacings are much smaller than in the case of $T_{\text{eff}} = 25$ nsec delay. Again it was verified that the fringe spacing was proportional to T_{eff}^{-1}. In comparison with Figs. 16 and 17, note the enormous gain in contrast associated with the traces of Figs. 21 and 23.

C. Extension to longer delays

Clearly, using this technique of phase modulation between alternate coherent pulse pairs, it should be possible to achieve a resolution much smaller than the natural linewidth of the excited state. The condition for this possibility is

$$(\text{Fringe spacing}) = \frac{1}{T_{\text{eff}}} = \frac{1}{2T} < \frac{1}{2\pi\tau_R} = \begin{pmatrix}\text{Natural linewidth of}\\ \text{the excited state}\end{pmatrix} \tag{30}$$

or

$$T_{\text{eff}} = 2T > 2\pi\tau_R . \tag{31}$$

Thus the effective delay between the two pulses must be longer than the radiative lifetime of the excited state multiplied by 2π.

For the case of the 4^2D excited state, $\tau_R \simeq 50$ nsec. Thus

$$2T > 2\pi \times 50 \text{ nsec}$$

or

$$T > 160 \text{ nsec} .$$

In order to obtain such a delay, one needs an ultrastable delay line with mirrors of ultrahigh optical quality, so that locking the center fringe of the two cw beams (direct and delayed) to the motion of the piezoelectrically driven mirror would become less troublesome. Also for such a long delay the wave-front curvature might be a serious problem; we have observed that when the wavefronts are not mode matched, the contrast of the fringes is reduced, and some asymmetry of the side fringes relative to the position of the central fringe develops. However, it is conceivable that all these difficulties could be overcome with a reasonable amount of effort. A more sophisticated detection system is needed, however, since the signal from the small number of longer-lived atoms might be hopelessly buried in laser fluctuations and detector noise.

Since our laser source is repetitively pulsed and the fluorescent decay photons necessarily appear within a few microseconds of the laser pulse, the output of the photodetector is averaged by a gated integrator system which accepts signals during limited time intervals. This technique eliminated most of the photomultiplier background without the need for cooling the detector, and eliminated as well spurious signals due to overhead lights, and the cw oscillating waves which were collinear with the pulses. Theoretically, the minimum detectable signal is then on the order of one photoelectron per laser pulse. In real experimental situations, however, various phenomena degrade the signal-to-noise ratio obtained by this method, making it impossible to observe the interference fringes. For instance, at the low signal levels involved, all materials fluoresce somewhat when excited by a laser, and care must be taken to shield the photodetector from such spurious radiation. Furthermore, undesirable fluorescence may result from linear absorption in the sample itself. Another problem is that many alkali metal vapors, for example, can form dimers capable of absorbing the frequencies needed for two quantum absorption in the atoms. Many of the excited molecules will then decay by fluorescing at wavelengths longer than the incident wavelength. However, some molecules may absorb a second quantum and dissociate into atoms, one of which may be significantly excited to radiate at an atomic line of wavelength shorter than the incident radiation.

If the detected fluorescence corresponds to a resonance line (as in our case for the detection of 4^2P–3^2S at 3302 Å), the phenomenon of self-absorption will result in the occurrence of the bulk of the fluorescence signal on the resonance line of longest wavelength, in violation of the expected branching ratios. Finally, one might encounter a situation in which *ac* Stark effect would wash out the interference signal. For example, when an accidental near-resonant or resonant enhancement is encountered, the pulse-to-pulse jitter can give rise to a random *ac* Stark shift from one pulse to the other. This could easily bury the interference signal for these long-lived atomic states.

All other techniques having failed, it is indeed possible to detect the interference signal on a single quantum event basis by interfacing the signal with an on-line computer, thus accumulating and averaging the data over a long period of data taking.

V. EXPERIMENTS WITH T VARYING

From Eq. (24), when ω_0 and ω are fixed and only T is varied, the result should be a sinusoidal variation with a period

$$\Delta T = 2\pi/\omega_0 . \tag{32}$$

If, however, the damping due to spontaneous emission between the two pulses is taken into account, then Eq. (24) can be written in the following form

$$b_2 = b_1[e^{-\Gamma T/2} + e^{i\omega_0 T}] \tag{33}$$

or

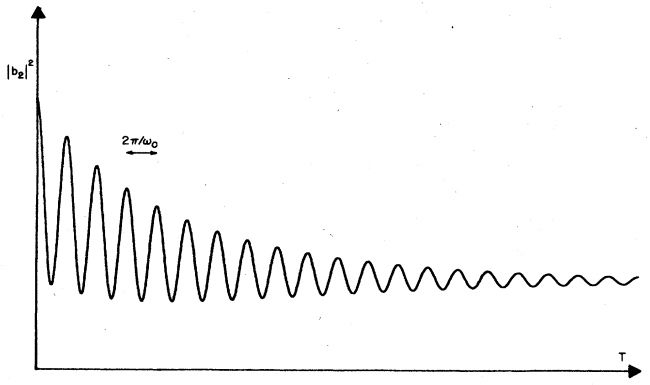

FIG. 24. $|b_2|^2$ [Eq. (33)] as a function of the delay time T.

$$|b_2|^2 = |b_1|^2[1 + e^{-\Gamma T} + 2e^{-\Gamma T/2}\cos\omega_0 T]. \quad (34)$$

Thus one should expect essentially a damped sinusoid, as illustrated in Fig. 24. The period of this sinusoid is related to the atomic frequency ω_0, and *not* the laser frequency ω. The variation ΔT of the delay line is directly related to the displacement $\Delta l = c\Delta T$ of the piezoelectrically driven mirror in the delay line (c: velocity of light); thus if, instead of plotting the signal versus T, one plots it versus l, the period of the sinusoid becomes:

$$2\pi c/\omega_0 = \lambda_0 . \quad (35)$$

Such an experiment could therefore provide a more direct measurement of the wavelength λ_0 of the atomic transition. The precision of the measurement is limited by the number of oscillations of the sinusoid of Fig. 24 (with optical period $2\pi/\omega_0$) during the radiative lifetime $1/\Gamma$. This technique thus provides in principle a Doppler-free method for measuring atomic wavelengths. It should be noted, however, that in order to take maximum advantage of this technique, it would be necessary to record a large number of oscillations, $\sim\omega_0/\Gamma$, which would require scanning the mirror over distances of the order of meters. Such an experiment would clearly be more difficult.

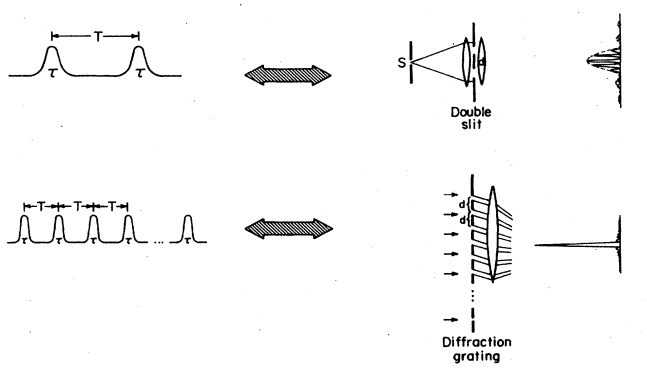

FIG. 25. Coherent time delayed two-pulse and multipulse signals and corresponding two- and multiple-slit interference patterns.

VI. CONCLUSION

In this paper we have introduced a technique which could mark the beginning of a new epoch in optical physics, where through the use of delayed pulses, pulse-length broadening can be overcome. Thus pulsed dye lasers, the only spectroscopic tool presently available in many spectral regions, can be used for ultrahigh-resolution spectroscopy of atomic and molecular systems. One can also consider situations where a coherent state is prepared by a two-photon resonant pulse at frequency ω_1 and subjected to a delayed probe pulse at frequency ω_2. A backward-going wave is thus generated in a four-wave mixing process at frequency $\omega_3 = 2\omega_1 - \omega_2$. The intensity of this wave gives a measure of the macroscopic coherence in the medium and the decay of the reflected intensity as a function of the delay should give a measure of the homogeneous dephasing of the two-photon state. This technique can be used to derive T_2, the collisions broadening factor, without the need of using a narrowband laser light source. This work marks a logical beginning of a stimulating and exciting new generation of optical experiments. Our technique can be generalized. Instead of two pulses, one could use a sequence of N equally spaced pulses (obtained, for example, by sending an initial pulse into a confocal resonator), and thus submit atoms to a series of N equally spaced time-delayed and phase-locked pulsed standing waves (Fig. 25). An argument parallel to the discussion of Figs. 2 and 3 would show that the optical analog of such a system is a grating with N lines; the total length of the grating corresponds to the total duration NT of the pulse train. In such a case, the frequency spectrum experienced by the atom would be a series of narrow peaks, N times narrower in width and N^2 times stronger in intensity, separated by a frequency interval T_{eff}^{-1}. Such narrow multipulse resonance lines have recently been observed by Teets *et al.* (1977) for the $3S$–$5S$ transition of atomic sodium with a very simple experimental setup. The pulse train is produced by injecting a single short dye-laser pulse into an optical cavity formed by two mirrors. The gas sample is placed near one end mirror so that the atoms see a pulsed standing-wave field once during each round trip, when the pulse is being reflected by the mirror. For spectral fine tuning the resonator length is scanned with a piezotranslator. The observed sharp multipulse interference fringes can be interpreted in terms of the modes of the optical resonator. The resolution is limited only by the natural atomic linewidth and by the losses of the resonator, not by the laser bandwidth.

The same scheme can provide a dramatic signal increase if the laser pulse is injected into the resonator without loss, for instance with some acousto-optic light switch. As long as atomic relaxation can be neglected, the probability of two-photon excitation for small intensities is proportional to the square of the number of pulse roundtrips; if the pulse recurs a hundred times, the two-photon signal will be 10^4 times stronger than in a single-pulse experiment. This enhancement can make it possible to use larger, less intense beams, reducing light shifts and transit-time broadening.

Two-photon excitation with multiple phase-coherent

light pulses promises to extend the range of Doppler-free laser spectroscopy to new wavelength regions, in particular the ultraviolet and vacuum ultraviolet, where only short-pulse laser sources are available at present.

Note added in proof (May 1978): During the past year, since this paper was submitted, considerable progress has been made in the application of quantum interference effects in two-photon spectroscopy. A brief summary should be given here. Bassini and co-workers (Bassini *et al.*, 1977) have demonstrated that in Doppler-free two-photon spectroscopy, due to compensation of the Doppler effect in a standing wave, it is possible to observe Raman scattering with the same detuning for all atoms (unlike single-photon excitation, where the detuning from the resonance in Raman scattering varies with the velocity, because of the Doppler shift). In particular they have observed, when the exciting light was switched on or off, transients corresponding either to resonance fluorescence (when the detuning was zero) or Raman scattering (when the detuning was larger than the natural width of the excited state). Similarly, Liao and co-workers (Liao *et al.*, 1977a) and Loy (1977) have applied the Stark switching technique to study transients both using a resonant intermediate state and using a non-resonant intermediate state for the two-photon transition.

As pointed out in our conclusion (see also Salour, 1977a, and 1978b, p. 499), by preparing atoms in a two-photon coherent state, using a two-photon resonant pulse at frequency ω_1, and subjecting them to a delayed probe pulse at frequency ω_2, one can generate a backward-propagating wave, in a four-wave mixing process, at frequency $2\omega_1 - \omega_2 = \omega_3$. This backward wave is phase conjugate to the probe and has recently been used for image conjugation (Bloom and Bjorklund, 1977). The intensity of this wave can give a measure of the macroscopic coherence in the medium, and the decay of the reflected intensity as a function of the delay gives a measure of the homogeneous dephasing of the two-photon state. Both Matsuoka (1975) and Liao (Liao *et al.*, 1977b) have proposed this, and Liao and co-workers demonstrated the technique, measuring the collision broadening factor using a broadband laser. Finally, Eckstein and co-workers (Eckstein *et al.*, 1978) have demonstrated the feasibility of Doppler-free two-photon spectroscopy with a train of picosecond standing-wave light pulses from a synchronously pumped mode-locked cw dye laser, and have thus observed a multi-pulse spectrum of the sodium $3s - 4d$ two-photon transition.

ACKNOWLEDGMENTS

I am deeply indebted to Professor C. Cohen-Tannoudji for much invaluable advice and constant enthusiasm on this work. I also wish to thank Professor N. Bloembergen, and my colleagues at Ecole-Normale Superieure (Paris), for many constructive discussions and a critical review of the original manuscript. Thanks are also due to P. H. Cox, L. Donaldson, R. W. Stanley, and D. A. Van Baak for expert technical assistance and for help in data taking.

REFERENCES

Abella, I. D., N. A. Kurnit, and S. R. Hartmann, 1964, Phys. Rev. Lett. **13**, 567.
Abella, I. D., N. A. Kurnit, and S. R. Hartmann, 1966, Phys. Rev. **141**, 391.
Alley, C. O., 1960, in *Quantum Electronics: A Symposium* edited by Charles H. Townes (Columbia University, New York), p. 146.
Arditi, M., and T. R. Carber, 1964, IEEE Trans. Instrum. Meas., IM-13(2), (3), p. 146.
Baklanov, Ye. V., B. Ya. Dubetskii, and V. P. Chebotayev, 1976a, Appl. Phys. **9**, 171.
Baklanov, Ye. V., B. Ya. Dubetskii, and V. P. Chebotayev, 1976b, Appl. Phys. **11**, 201.
Bassini, M., F. Biraben, B. Cagnac, and G. Grynberg, 1977, Opt. Comm. **21**, 263.
Belenov, E. M., and I. A. Poluektov, 1969, Zh. Eksp. Teor. Fiz. **56**, 1407 [Sov. Phys.-JETP **29**, 754 (1969)].
Bergquist, J. C., S. A. Lee, and J. L. Hall, 1977, Phys. Rev. Lett. **38**, 159.
Bloom, D. M., and G. C. Bjorklund, 1977, Appl. Phys. Lett. **31**, 592.
Brewer, R. G., and E. L. Hahn, 1975, Phys. Rev. A **11**, 1641.
Cagnac, B., G. Grynberg, and F. Biraben, 1973, J. Phys. (Paris) **34**, 56.
Cagnac, B., G. Grynberg, and F. Biraben, 1974, Phys. Rev. Lett. **32**, 645.
Chebotaev, V. P., A. V. Shishayev, B. Ya. Yurshin, and L. S. Vasilenko, 1978, Appl. Phys. 15, 43.
Clark, B. O., D. A. Van Baak, and F. M. Pipkin, 1977, Phys. Lett. A **62**, 78.
Dubetskii, B. Ya., 1976, Kvant. Elektron. (Moscow) **3**, 1258 [Sov. J. Quantum Electron. **6**, 682 (1976)].
Eckstein, J. N., A. I. Ferguson, and T. W. Hänsch, 1978, Phys. Rev. Lett **40**, 847.
Fled, M. S., and V. S. Letokhov, 1973, Sci. Am. (December), p.69.
Grischkowsky, D., 1970, Phys. Rev. Lett. **24**, 866.
Grischkowsky, D., M. M. T. Loy, and P. F. Liao, 1975, Phys. Rev. A **12**, 2514.
Grove, R. E., F. Y. Wu, L. A. Hackel, D. G. Youmans, and S. Ezekiel, 1973, Appl. Phys. Lett. **23**. 442.
Hänsch, T. W., K. Harvey, G. Meisel, and A. L. Schawlow, 1974, Opt. Commun. **11**, 50.
Hartig, W., and H. Walther, 1973, J. Appl. Phys. **1**, 171.
Hartmann, S. R., 1968, IEEE J. Quantum Elect. **QE-4**,802.
Hocker, G. B., and C. L. Tang, 1968, Phys. Rev. Lett. **21**, 591.
Hocker, G. B., and C. L. Tang, 1969, Phys. Rev. **184**, 356.
Levenson, M. D., and N. Bloembergen, 1974, Phys. Rev. Lett. **32**, 645.
Li, M. C., 1977, Nuovo Cimento, **39B**, 165 (1977).
Liao, P. F., J. E. Bjorkholm, and J. P. Gordon, 1977a, Phys. Rev. Lett. **39**, 15.
Liao, P. F., N. P. Economou, and R. R. Freeman, 1977b, Phys. Rev. Lett. **39**, 1473.
Loy, M. M. T., 1974, Phys. Rev. Lett. **32**, 814.
Loy, M. M. T., 1977, Phys. Rev. Lett. **39**, 187.
Matsuoka, M., 1975, Opt. Commun. **15**, 84.
Mössbauer, R. L., 1958a, Z. Phys. **151**, 124.
Mössbauer, R. L., 1958b, Naturwissenschaften **45**, 538.
Mössbauer, R. L., 1959, Z. Naturforsch. **14a**, 211.
Pound, R. V., and J. L. Snider, 1965, Phys. Rev. **140**, B788.
Ramsey, N. F., 1949, Phys. Rev. **76**, 996.
Ramsey, N. F., 1956, *Molecular Beams* (Oxford University, New York).
Salour, M. M., 1976a, Bull. Am. Phys. Soc. **21**, 1245.
Salour, M. M., 1976b, Opt. Commun. **18**, 377.
Salour, M. M., 1977a, Ph. D. thesis (Harvard), unpublished.
Salour, M. M., 1977b, Appl. Phys. Lett. **31**, 394.
Salour, M. M., 1977c, Opt. Commun. **22**, 202.
Salour, M. M., 1978, Phys. Rev. A **17**, 614.
Salour, M. M., and C. Cohen-Tannoudji, 1977, Phys. Rev. Lett. **38**, 757.

Salour, M. M., 1978b, Annals of Physics **111**, 364.
Snyder, J. J., and J. L. Hall, 1975, in *Laser Spectroscopy*, edited by S. Haroche, J. C. Pebay-Peyroula, T. W. Hänsch, and S. E. Harris (Springer, Heidelberg).
Takatsuji, M., 1971, Phys. Rev. A **4**, 808.
Takatsuji, M., 1975, Phys. Rev. A **11**, 619.
Teets, R., J. Eckstein, and T. W. Hänsch, 1977, Phys. Rev. Lett. **38**, 760.
Treacy, E. B., 1968, Phys. Lett. A **27**, 421.
Treacy, E. B., and A. J. DeMaria, 1969, Phys. Lett. A **29**, 369.
Vasilenko, L. S., V. P. Chebotayev, and A. V. Shishaev, 1970, Zh. Eksp. Teor. Fiz. Pis'ma Red. **12**, 161 [JETP Lett. **12**, 113 (1970)].
Weingarten, R., 1972, Ph. D. thesis (Columbia), unpublished.
Woerdman, J. P., 1976, Chem. Phys. Lett. **43**, 279.